

## Microscopic charcoals in ocean sediments off Africa track past fire intensity from the continent

Aritina Haliuc<sup>1,6,7</sup>, Anne-Laure Daniau<sup>1</sup>, Florent Mouillot<sup>2</sup>, Wentao Chen<sup>2</sup>, Bérangère Leys<sup>3</sup>, Valérie David<sup>1</sup>, Vincent Hanquiez<sup>1</sup>, Bernard Dennielou<sup>4</sup>, Enno Schefuß<sup>5</sup>, Germain Bayon<sup>4</sup> & Xavier Crosta<sup>1</sup>

Fires in Africa account for more than half of global fire-carbon emissions but the long-term evolution of fire activity and its link to global climate change remains elusive. Paleofire records provide descriptive information about fire changes through time, going beyond the range of satellite observations, although fire regime characteristics are challenging to reconstruct. To address this conceptual gap, we report here the abundance and morphometric data for a large set of microscopic charcoal samples ( $n = 128$ ) recovered from surface ocean sediments offshore Africa. We show that in subtropical Southern Africa, large and intense fires prevailing in open savanna-grassland ecosystems produce a high abundance of small and elongated microcharcoal particles. In contrast, in the forest ecosystems of equatorial and tropical regions of western and central Africa, low-intensity fires dominate, producing low amounts of squared microcharcoal particles. Microcharcoal concentration and morphotype in marine sediment records off Africa are thus indicative of fire regime characteristics. Applied to down-core marine charcoal records, these findings reveal that at orbital time-scale intense and large, open grassland-savanna fires occurred during wet periods in the sub-tropical areas. A strong contribution of fire carbon emissions during periods of precession and summer insolation maxima in the geological record is thus expected.

<sup>1</sup>University Bordeaux, CNRS, Bordeaux INP, EPOC, UMR 5805, F-33600 Pessac, France. <sup>2</sup>UMR CEFE, University Montpellier, CNRS, EPHE, IRD, Univ. Paul Valéry Montpellier 3, 1919 route de Mende, 34293 Montpellier, CEDEX 5, France. <sup>3</sup>Aix Marseille University, Avignon University, CNRS, IRD, IMBE, Aix Technopole de l'environnement Arbois Méditerranée Avenue Louis Philibert - Batiment Villemin, 13545 Aix-en-Provence, Cedex 4, France. <sup>4</sup>University Brest, CNRS, Ifremer, Geo-Ocean, F-29280 Plouzané, France. <sup>5</sup>MARUM - Center for Marine Environmental Sciences, University of Bremen, Leobener Strasse 8, 28359 Bremen, Germany. <sup>6</sup>Present address: Stefan Cel Mare University of Suceava, MANSiD, Universitatii 13, 720229 Suceava, Romania. <sup>7</sup>Present address: Romanian Academy, Institute of Speleology, 5 Clinicilor, Cluj-Napoca 400006, Romania. ✉email: [aritinahaliuc@gmail.com](mailto:aritinahaliuc@gmail.com); [anne-laure.daniau@u-bordeaux.fr](mailto:anne-laure.daniau@u-bordeaux.fr)

Fire has shaped ecological systems for millions of years and represents one of the most important causes of environmental disturbances on Earth, playing key roles in global biogeochemical cycles, ecosystem patterns and processes<sup>1–4</sup>. Satellite records demonstrate that more vegetation is burning in Africa than anywhere else on Earth. Fires there account for more than 50% of fire-related carbon emissions worldwide and more than 70% of the global burnt area. Africa hence holds the most fire-prone ecosystems, where fire plays a major role in the global interannual variability of greenhouse gases<sup>4</sup>.

Fire change projections are largely uncertain, especially in Africa<sup>5</sup> where statistical models predict either a decrease<sup>6</sup> or an increase<sup>7</sup> in the same area for the forthcoming century. These empirical relationships are developed using data covering the instrumental period and, therefore, neglect potential changes in interactions and feedbacks between climate, vegetation and fire beyond the range of modern observations. Because the projected climate change far exceeds the time-scale of instrumental or air/borne observations, process-based models of the coupled vegetation–fire system are used. However, they still need to be evaluated and benchmarked using paleofire data<sup>8</sup>. We rely, therefore, on natural archives to reconstruct long-term fire regime changes under different climate conditions for future scenarios<sup>9–13</sup>. Sedimentary charcoal records provide an estimate of the changes in fire activity or biomass burning and have the potential to offer quantitative measurements directly comparable to simulated values of the fire regime parameters such as fire number, size, frequency, and intensity<sup>11,14–16</sup>. However, despite the efforts of the paleofire international community, we are still missing comprehensive fire-proxy calibrations<sup>8,11,14–16</sup>. Numerous charcoal calibration studies on terrestrial sediment records suggested a positive relationship between charcoal accumulation and one of the physical parameters of the fire regime, i.e., burnt area<sup>14–20</sup>, intensity<sup>14,15</sup>, fire number<sup>14,21</sup> and severity<sup>22</sup>. Charcoal preserved in marine records is used to reconstruct regional fire activity. It also provides indirect information about hydroclimate and vegetation changes through time<sup>23</sup> as fire is controlled by climate and vegetation. Previous works on the long-term fire history in subtropical African regions highlighted a monsoon control on fire activity at orbital timescales through fuel development. For example, an increase in fire activity was observed in northwestern Africa during the humid early Holocene when high savanna biomass was reconstructed<sup>24</sup>, and in southern Africa during the Late Quaternary when periods of precession and austral summer insolation maxima enhanced grass-<sup>23</sup> and fynbos-fueled fires<sup>25</sup>. In the marine environment, a few published calibration studies have linked charcoal accumulation and morphotypes with burnt area and fire intensity in California<sup>26</sup> and the Iberian Peninsula<sup>27</sup>. In addition, previous work has shown that the distribution pattern of charcoal concentrations correlated with charcoal influx in North Pacific marine sediments<sup>28</sup>, suggesting that charcoal distribution patterns in sediments are not controlled by any dilution effect but instead faithfully reflect the sedimentary flux of charcoal particles. Nevertheless, there are still important limitations in relating fire proxies from natural records with fire regime characteristics. This is due to the different temporal and spatial resolution between natural archives and instrumental records, the diverse charcoal amount produced during combustion, the difficulty of tracing charcoal source area and various taphonomic processes<sup>11</sup>. The first inferences of fire regime characteristics from marine paleofire records were derived using indirect theoretical principles developed on charcoal from lake sediments and experimental studies. A peak in microcharcoal concentration or influx was interpreted as an increase in fire frequency and intensity while the particle shape was used to infer intensity and vegetation type. Recently, it has been demonstrated

that charcoal abundance and morphotype in marine surface sediments off Iberia can trace specific fire regimes on land, in particular fires of high intensity in a mixed open Mediterranean woodland vegetation<sup>29</sup>. However, there is no empirical data yet to support paleofire regime inferences made from marine microcharcoal records off Africa.

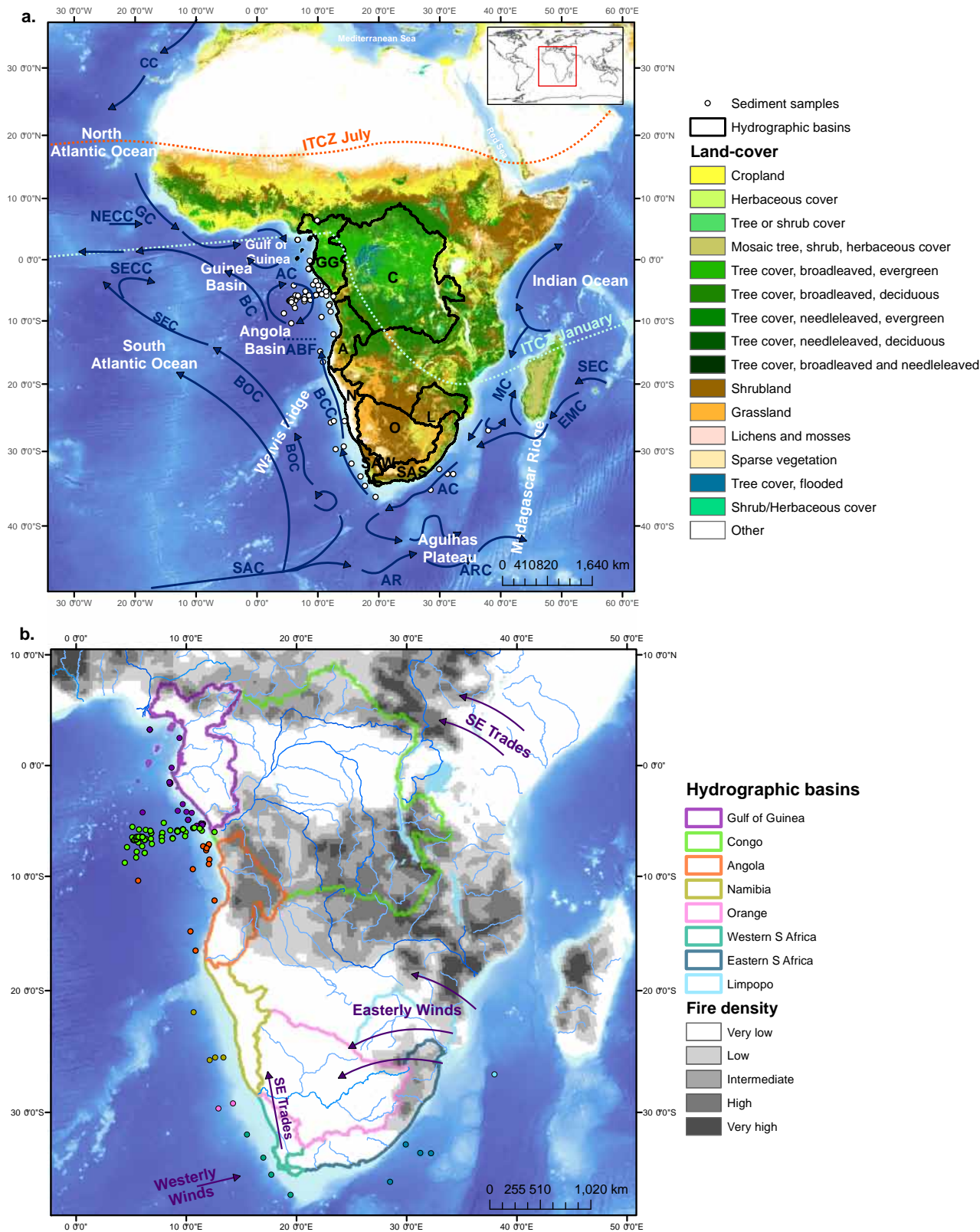
Here, we aim to explore the relationships between microscopic charcoal (microcharcoal) characteristics preserved in recent marine sediments along the Atlantic margin off (sub)-tropical Africa (Fig. 1a) and the changes in fire regimes in adjacent regions. To this purpose, we determined the abundance and morphotypes of microcharcoal in surface sediments and compared the obtained data with satellite-derived fire information (fire number, size, intensity and type of burnt vegetation) over the recent period. Based on these results, we propose a new framework linking microcharcoal accumulation and morphometric values in marine sediments to burned vegetation types and fire regimes for Africa. We apply this framework to marine charcoal records located off subtropical African regions to discuss changes in the paleofire regimes over a multimillennial timescale.

## Results

**Distribution pattern of sedimentary charcoal in seafloor sediment.** Microscopic charcoal particles, between 10 and 92  $\mu\text{m}$  in length, were extracted from surface (core-top) marine sediment samples ( $n = 128$ ; Material and Methods) collected at the African Atlantic margin, from the Gulf of Guinea to the Cape Basin, and on the Indian side, from the Agulhas Plateau to the Limpopo region (Fig. 1a). We analyzed the concentration and morphometric characteristics of microcharcoal, including area, length, width and elongation (length/width ratio), to examine charcoal distribution patterns in ocean sediments and their relationships with fire regimes on land.

Following vegetation burning, microcharcoal particles are released and transported with the fine-grained sediment fraction to the ocean, via fluvial systems or aerial dispersion<sup>29</sup> (SI Section 1). Given the size and weight of microcharcoal particles, ranging between  $>10 \mu\text{m}$  and  $<100 \mu\text{m}$  in length<sup>30</sup>, they behave similarly to pollen and fine terrigenous particles during transport and sedimentation<sup>31</sup>. In marine sediments proximal to river plumes, fine terrigenous particles are primarily of fluvial origin<sup>32,33</sup>. Only off arid regions, where no hydrographic system is present, the aeolian transport can represent the dominant carrier of fine particles<sup>34</sup>. In the ocean, fine particles become an integral part of the marine snow, reaching the sea floor within a few days or weeks<sup>35,36</sup>. In addition, the latitudinal pollen distribution in marine surface sediments represents faithfully the vegetation distribution on the adjacent continent<sup>32,35,37–39</sup>. Although microcharcoal and pollen share similar fluvial behaviour during fluvial transport, they however behave slightly differently during aerial dispersal due to differing physical-mechanical characteristics<sup>40</sup>. In this study, we therefore evaluated the potential contribution of windblown microcharcoal particles using a dispersion and deposition model (see Material and Methods and SI Section 3) showing that wind and fluvial source areas overlap so that most of charcoal produced in one hydrographic basin is deposited in the same basin and can then be transported to the ocean by the fluvial system.

Consequently, we defined eight regional source areas for sedimentary microcharcoal, roughly based on the proximity to the river system entering the ocean, i.e., Gulf of Guinea, Congo, Angola, which represent the central western Africa region, Namibia, Orange, western South Africa (WSA), Eastern South Africa (ESA) and Limpopo which represent Southern Africa (Fig. 1a). Charcoal preserved in samples off southern Africa (the



southern area of study) reflects therefore fire activity of subtropical Africa and charcoal preserved in samples off central western Africa reflects the fire activity of equatorial/tropical Africa. Samples located off the Gulf of Guinea, Orange and WSA share similar, relatively low mean microcharcoal concentration values, below 100,000 nb.g<sup>-1</sup> (Fig. 2). Intermediate mean microcharcoal values, between 100,000 and 200,000 nb.g<sup>-1</sup> are

typical for Angola, Congo but also Namibia and WSA. The highest microcharcoal concentration value is attained by the sample located off Limpopo (Fig. 2). Samples located off Namibia, Orange, WSA and Limpopo show higher mean elongation ratio (>1.8) whereas samples located off Gulf of Guinea, Angola, Congo and ESA coast display values <1.8 (two-tailed *t*-test, *p* < 0.05) (Fig. 2).

**Fig. 1 Study area characteristics and ocean sediment sample location.** **a** Study area with main vegetation types following ESA-CCI (Supplementary Table 2), ocean currents and location of ocean sediment samples analyzed and the studied hydrographic basins with abbreviated names (GG Gulf of Guinea; C Congo; A Angola; N Namibia; O Orange; L Limpopo; SAW South Africa West; SAS South Africa South). GC Guinea Current; SEC South Equatorial Current; EUC Equatorial Under Current; SECC South Equatorial Counter Current; AC Agulhas Current; ARC Agulhas Return Current; EMC East Madagascar Current. **b** The location of ocean sediment samples (dots) color-coded based on the preferential microcharcoal source area (areas on land) with fire density (calculated from the FRY 2 version as the mean yearly fire number) and major wind direction. The maps were created in ArcMap version 10.8.1. The background map was downloaded from European Space Agency (ESA) Climate Change Initiative (CCI) Land Cover (LC) database<sup>77</sup> and ArcGIS Online. The fire density was generated using the FRY dataset global fire patch database.

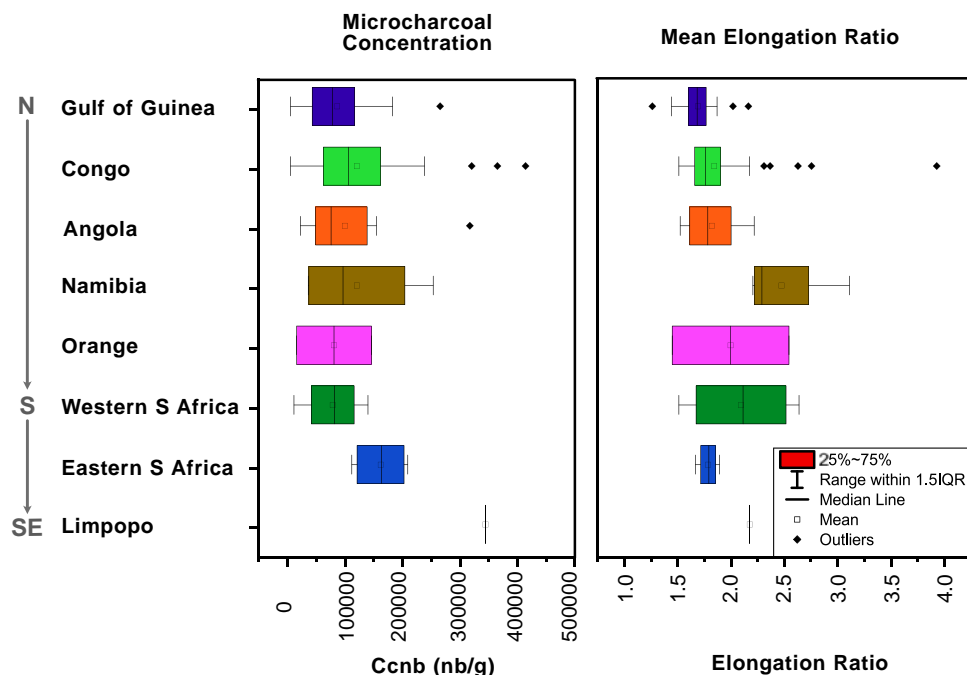


**Fig. 2 Microcharcoal results derived from surface marine sediment sample.** Boxplots of mean microcharcoal concentration and mean elongation ratio derived from marine sediment samples in each zone.

We applied principal component analysis (PCA) on mean ocean charcoal parameters, including concentration, elongation, width, area and length, to identify the association between parameters and potential clustering of charcoal particle types (Fig. 3a). The first two components of the PCA on the mean charcoal (concentration, elongation, width, area and length) per hydrographic basins explain almost 80% of the overall variance of the mean data (Fig. 3a). PC 1 is correlated with area, length and width of charcoal particles, and PC 2 is correlated with charcoal elongation and concentration strength,  $\cos^2 > 0.5$ , Fig S.5. The PCA results show high heterogeneity in the distribution of samples. However, strong relationships between charcoal abundance and morphotype were established among the different hydrographic basins and between western central and southern Africa (Fig. 3a, Kruskal–Wallis tests,  $p < 0.05$ ). The Kruskal–Wallis test applied on PC2 (correlated with concentration and elongation) shows evidence for significant differences between basins (Kruskal–Wallis chi-squared = 21.199,  $df = 7$ ,  $p$ -value = 0.003486) as well as a significant difference between the two main regions (Kruskal–Wallis chi-squared = 8.1685,  $df = 1$ ,  $p$ -value = 0.004262). At sub-continental scale, microcharcoal patterns in marine sediments off Africa are described by two main variables, elongation and concentration. The shape and size of microcharcoal particles group together samples from Namibia, Orange and SAW (southern Africa - southern region), whereas the shape of particles groups samples from Congo, Angola and Gulf of Guinea basins (western central Africa). Samples from western central Africa correspond to squared particles of variable

size present in low concentration in the sediment. In contrast, most samples from Southern Africa are characterized by small, elongated particles in high concentration (Fig. 3a).

**Charcoal concentrations and morphotypes informing fire regime changes.** To identify the potential link between charcoal accumulated in the ocean and fire on land, we compared the detected patterns for marine sedimentary charcoal with various parameters of fire regimes on adjacent continental regions (Fig. 3b). PCA was applied on land fire parameters including number of fires (Nb fires), mean fire radiative power (FRP), area, rate of spread (RoS) and the burnt vegetation types (graminoid - G, mixed - M and trees - T) to characterize the fire regime specific for each hydrographic basin (Fig. 3b). We used the mean FRP in  $W.m^{-2}$  as a measure of fire intensity. The FRP index measures the energy emitted through radiative processes released during the combustion and can be associated with fire intensity throughout the fire-burning process<sup>41</sup>. Principal component axis 1 explains 32%, and axis 2 explains 23% of the variance in all variables. PC 1 opposes FRP and mixed burnt vegetation to burnt trees, while PC2 opposes RoS to burnt graminoids (Supplementary Fig. 5). Samples from Congo, Angola and the Gulf of Guinea tend to cluster on the positive values of PC 1 and are associated with burnt trees. Samples from Orange, SAW and Namibia are found in the negative part of PC 1 and are associated with FRP, burnt mixed, RoS and mixed burnt vegetation to burnt trees, while PC2 opposes RoS to burnt graminoids (Supplementary Fig. 5). The Kruskal–Wallis test shows that fire regimes in each hydrographic basins

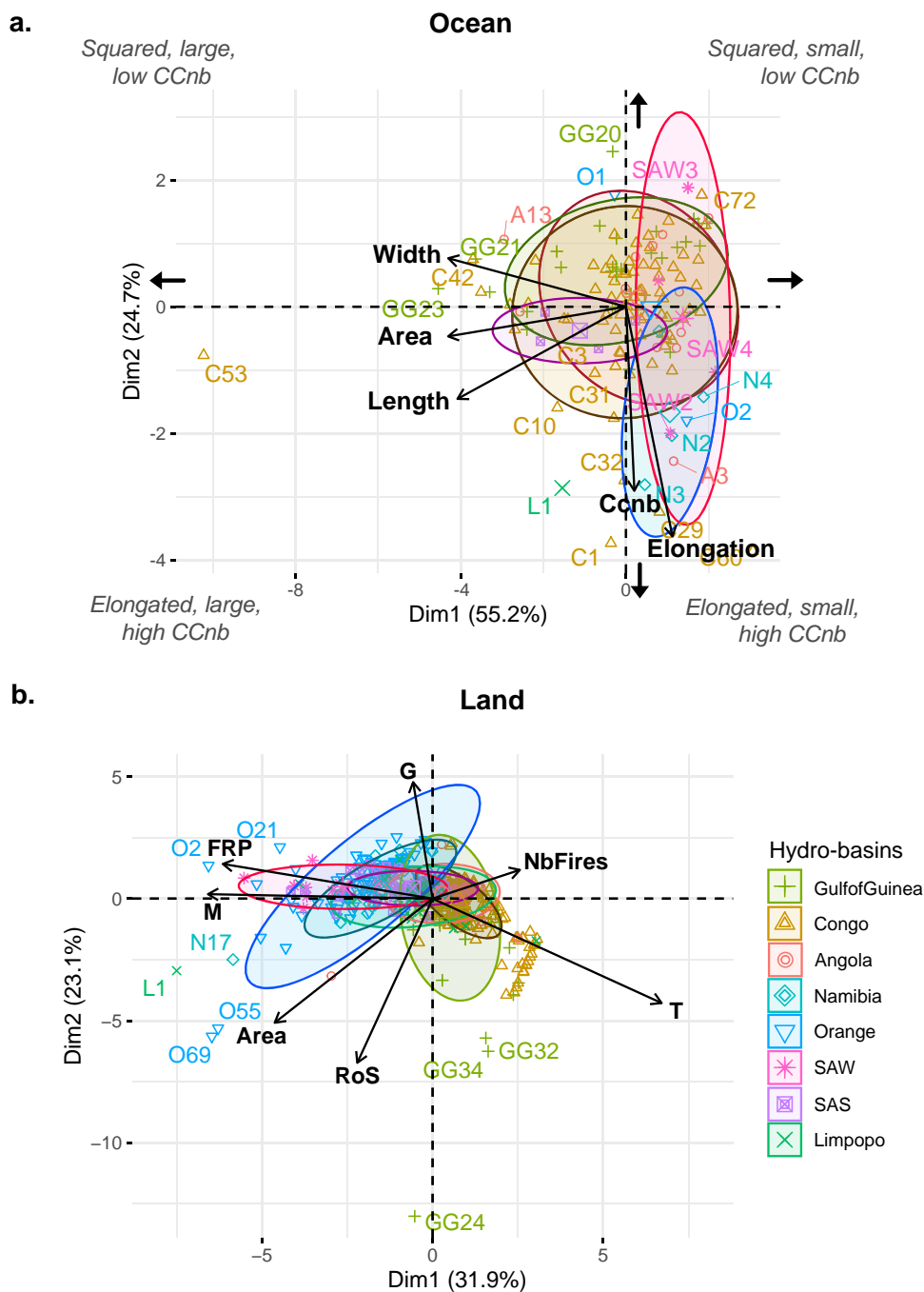


**Fig. 3 Statistical results on microcharcoal assemblages from ocean sediment samples and land fire data. a** Results of the principal component analysis on microcharcoal assemblages including length, area, width, elongation and charcoal concentration (Ccnb) with the interpretation of the four spaces defined. **b** Principal component analysis on land fire parameters (derived from FRY2 version at 1° × 1° grid) including fire number, area (ha), mean fire radiative power (FRP, W/m<sup>2</sup>), rate of spread (RoS) for major burnt vegetation types (G Graminoids, M Mixed, T Trees). Ellipses with different colors and symbols represent the hydro-basins (please note that Namibia and Limpopo do not form an ellipse on the ocean data due to the restricted number of samples). The legend for the eight hydrographic basins (colors and symbols) are presented on the right side of the chart. Graminoids correspond to grassland-savanna vegetation, and trees correspond to woodland vegetation.

(Kruskal–Wallis chi-squared = 419.37, df = 7, *p*-value = 0.000) and between distinct regions, i.e., western central and Southern Africa, are statistically different (Kruskal–Wallis chi-squared = 13.626, df = 1, *p*-value = 0.0002231). Our assessment of African fire regimes (PCA) indicates that small (local) fires of low intensity occurring in tree-dominated areas mostly prevail in western central Africa, whereas large (more regional) fires of high intensity and high rate of spread involving mixed, graminoid-

shrub vegetation are mostly encountered in southern Africa (Fig. 3). Taken together, our results indicate that low amounts of charcoal particles with squared shape are observed in marine sediments proximal to regions dominated by small fires of low intensity in tree-dominated ecosystems, whereas larger amounts of small charcoal particles with elongated shape are observed in proximity to landscapes experiencing large and high-intensity fires in graminoid-mixed ecosystems<sup>32</sup>.

## Discussion

Some relationships between charcoal accumulation or morphotypes and individual fire parameters have been previously documented at local scales in lake records from various climatic and vegetation settings, i.e. boreal<sup>22</sup>, temperate<sup>14</sup> to grass-ecosystems<sup>18,42</sup>, as well as in marine sediments<sup>26,27</sup>. More specifically, a similar approach<sup>27</sup> albeit at a smaller spatial scale and restricted to temperate and Mediterranean fire ecosystems of the Iberian Peninsula, reported higher charcoal concentration and elongation values in marine samples associated with fires spreading in open Mediterranean woodlands in Iberia<sup>27</sup>. Here, we demonstrate at a larger sub-continental scale and for environmental settings ranging from tropical to subtropical climate, tropical to desert biomes, that concentration and elongation of charcoal in marine sediments off Africa can be used to identify different fire regimes. At this sub-continental scale, it is difficult to argue that transport and/or sedimentation processes mostly control the observed distribution pattern of sedimentary charcoal in seafloor sediments. Instead, previous studies have shown that the amount of charcoal is generally controlled by production source characteristics such as fuel type, biomass, fire size and intensity<sup>43,44</sup>.

A possible explanation for the observed distribution pattern of charcoal morphotypes (concentration, shape and size) could result from different transport mechanisms between regions influenced by grain-size sorting during eolian transport and others dominated by river discharge, or by surface ocean circulations. However, all regions combine the influence of large river basins (Congo and Orange rivers) and intense ocean currents (BCC and AC, Fig. 1a), and prevailing southeasterly trade winds. Another possibility lies in a higher sediment export concentrating charcoal in preferential areas. However, both the Benguela upwelling system and the Congo fan are high sedimentation accumulation systems. Consequently, it seems unlikely that sediment transport processes control the observed latitudinal distribution pattern of charcoal in seafloor sediment.

The high charcoal concentrations observed in the marine samples off Southern Africa are associated with large fires of high-intensity spreading in graminoid-mixed vegetation i.e., open grassland-savanna ecosystems. Here, the graminoid-mixed vegetation is composed of a mixture of shrubland, grassy semi-desert and arid-fertile savanna, fynbos (winter rainfall shrubland) and vlei/dambo (seasonally-dry wetlands), leading to exceptionally high-intensity fires<sup>45</sup>. Rare, intense and large fires dominate the African savannas at its driest range<sup>46</sup>, with fuel availability limited for several years but sufficient and continuous during the rare wettest years to support large fires. Fires of high intensity consume more vegetation and burned large areas in southern Africa<sup>15</sup>. Such a relationship between high charcoal accumulation and high-intensity fires has been identified locally in several water bodies from the boreal region<sup>22</sup> and from the Kruger National Park<sup>15</sup> and in marine sediments off Iberia<sup>27</sup>. Our findings are consistent with the previous work suggesting that charcoal accumulation in sedimentary records reflects a shift in fire regimes rather than a change in a single fire parameter such as fire size, intensity, or frequency<sup>30</sup>.

Higher biomass availability in forested ecosystems was suggested to be the main parameter explaining higher charcoal accumulation in lacustrine sediments<sup>47</sup> or elemental carbon accumulation in marine proximal sediments<sup>48</sup>. However, the fuel load is low in subtropical African grasslands and savannas<sup>49</sup>, thereby arguing against control of overall biomass availability on the concentration of sedimentary charcoal in nearby sediments. Conversely, it has been shown that savanna fires consume leaves at 95% but wood only at 5 to 50%<sup>10</sup>. Therefore, the fuel material combusted by fires might exert a strong control on charcoal amount. In this vein, we propose that the intensity of wildfires in

Africa plays a major role in controlling the distribution patterns of associated sedimentary charcoal particles. This finding is fully consistent with some experimental studies showing a positive correlation between the amount of charcoal particles and fire intensity<sup>15,22,31,50,51</sup>. In addition, based on the combustion continuum, the size of charcoal is reduced from cm to micron scale with increasing temperature<sup>52</sup>. We thus infer that the high proportion of small-sized (microscopic) charcoal particles observed in Southern Africa results from high intensity fires due to the high burning temperature of fine fuel (grasses and leaves) which produces high fire emission (gases)<sup>4,49</sup>. Our results also demonstrate that the burning of herbaceous fuels produces much smaller particles than the woody fuels. However, our findings contrast with the experimental work suggesting that low-temperature surface fires produce more elongated particles than high-temperature fires<sup>53</sup>. This opposite trend is not surprising considering the different biogeographical regions (Africa vs Siberia) corresponding to vegetation types/plant associations (grassland-savanna vs boreal forests) in which fire behaviour and charcoal production and type are expected to differ significantly.

Experimental studies showed that charcoal particles produced by graminoid and graminoid-shrub burning (median elongation ~3) are more elongated than particles derived from the burning of tree and (sub)shrub (median elongation ~2)<sup>54</sup>. Results on the mean morphology of charcoal in our marine sediment samples suggest that southern African fires spread in mixed-graminoid vegetation (high mean elongation values of charcoal samples), whereas western central Africa is marked by forest fires (low mean elongation of charcoal samples) (Fig. 3a and b). This confirms our ocean-land comparison in terms of burnt vegetation type. Our data present much smaller mean elongation values (~<2.5) than those synthesized by experiments<sup>55</sup>. We argue that this difference arises from the fact that<sup>54</sup> compiled elongation data from the burning of a single type of vegetation (grassland and woodland). However, this is rather unrealistic for in-situ environments where fires spread across different vegetation and species types<sup>55</sup>. In samples from central and southern Africa charcoal assemblage (at sample level) is likely composed of particles coming from different burnt vegetation types and species. Another possible explanation for the observed smaller mean elongation values in our sedimentary charcoal samples could be related to the physical breakdown of charcoal into smaller grain-size with increasing distance of fluvial transport.

Thus, we propose a mean elongation classification at charcoal assemblage level to infer burnt vegetation type from charcoal in marine sediments (Supplementary Fig. 8). A value of  $<1.8 \pm 0.3$  representing tree burning is obtained by calculating the mean charcoal elongation for samples belonging to central western Africa. A value of  $>2.1 \pm 0.5$  obtained from Southern Africa charcoal samples tracks the burning of graminoids-mixed vegetation. Mean charcoal elongation from central western Africa is significantly different from values from southern Africa (*t*-test,  $p < 0.05$ ) (Supplementary Fig. 8). The threshold value of ~2 obtained here using the length/width ratio is in line with results from<sup>41</sup> tropical grassy ecosystems<sup>41</sup> and<sup>53</sup> from grass prairie ecosystems of North America<sup>53</sup>. These studies showed that a width/length ratio of 0.5 or less (an inverse length/width ratio  $>2$ ) characterize the burning of grassland-dominated vegetation, while values  $>0.5$  represent the combustion of ligneous vegetation (including both shrubs and trees).

At sub-continental scale, our results clearly show that micro-charcoal assemblages in marine sediments depend on the type of fire regimes on adjacent continental margins. As fires are expected to change predictably along climate-environmental gradients<sup>56</sup> such a relation provides a valuable source of information about fire-biome shifts over different time scales.

Previous work on paleofire in subtropical Africa suggested that at orbital scale the monsoon controls the fire activity through fuel development. In a marine sediment record off southwest Africa (MD96-2098<sup>23</sup>), higher microcharcoal concentration and more elongated particles were reported for glacial periods and during austral summer insolation maxima between 170 ka to 35 ka. These changes were interpreted as reflecting increasing fire activity during cool and wet periods associated with increasing grassland biomass. Under the same configurations (glacial times and austral summer insolation maxima), another study<sup>25</sup> showed high microcharcoal concentrations associated with fynbos expansion in a 300 ky-long (Site U1479) marine sedimentary record off south-western South Africa, which they interpreted as reflecting fynbos fires. In northern Africa higher microcharcoal concentration was reported during the early humid Holocene in core GeoB7920-2 associated with grass-savanna expansion<sup>24</sup> and interpreted as higher fire occurrence.

The modern land-ocean relationship proposed in this study helps interpreting the three marine charcoal records in terms of past fire regime changes (Fig. 4). In the marine sedimentary core off Namibia<sup>23</sup>, the high microcharcoal concentration associated with high elongation values at times of monsoon enhancement (austral summer insolation maxima) were interpreted as an increase in grass fires of low intensity. Our mean elongation classification applied on the long sedimentary core MD96-2098 suggests that in addition to grass fires<sup>23</sup>, mixed-fuel fires were also occurring. Based on our modern fire land data, contrary to previous interpretations, we suggest that the fires in southern Africa were of high intensity. We propose therefore an alternative interpretation and suggest that those increases in subtropical regions of Africa indicate a fire regime characterized by large fires of high intensity spreading in graminoid-mixed vegetation. Grass-fueled fires of low intensity were inferred on the basis of data for fire characteristics in sites located outside Africa<sup>23</sup>, under different environmental settings, which could explain the observed bias in interpretation. Looking at southwestern South Africa we propose that over the past 300 ky increased charcoal concentration at times of fynbos expansion revealed intense and large fires but not necessarily frequent fires<sup>25</sup>. In northwestern Africa, our land-ocean relationship suggests that fires were large during the humid early Holocene and not numerous<sup>24</sup>.

In summary, microcharcoal concentration and elongation from ocean sediment samples off the African coast portray the fire regime changes on land. On the one hand, high amounts of small and elongated charcoal track intense and large fires spreading into open grassland-savanna vegetation. On the other hand, low amounts of squared charcoal indicate small fires of low intensity, spreading in tree-dominated ecosystems. Among key processes, fire intensity appears to be the most important driver of charcoal morphotypes and abundance in Africa. Our work has important implications for charcoal calibration efforts developed by the international paleofire community. Our study shows that charcoal preserved in marine sediments off Africa is a valuable proxy to trace past open grassland-savanna fires and inform us about their variability, controls, and response to climatic changes. At the orbital timescale, our results suggest that intense and large open grassland-savanna fires occur during wet periods in subtropical regions of Africa. These intense fires might have been a source of carbon to the atmosphere during periods of precession and summer insolation maxima in the geological record. However, more geological data as well as model simulations, are necessary to quantify the contribution of fires to the atmospheric carbon cycle over orbital timescale.

### Material and methods

Different types of corers were used to retrieve the sediments including gravity, piston and box corer during different marine cruises including CONGOLOBE 2011<sup>57</sup>, ZAIANGO set of cruises run between 1998 and 2001<sup>58–60</sup>, RV Tyro 1989<sup>61</sup> and MD105 Images II NAUSICAA<sup>62</sup>. Samples were collected from the top 0 to 1 cm of these sediment cores stored in different repositories (EPOC and IFREMER, France) or obtained from PIs personal repositories. The samples are spread across different depositional settings, from estuary (1 sample), the continental shelf (1 sample), the continental slope (51 samples) to the abyssal plain (75 samples).

**Sample ages.** Chronological information was extracted from published studies for our core-top samples showing the samples cover less than two decades to a few or several centuries of environmental changes (please see Data availability). Thirty samples are dated less than 50 years, 20 less than 100 years,

### Fire regimes on land

Small, low intensity fires in tree-dominated vegetation



Large, intense fires in graminoid-mixed vegetation



### Charcoal in ocean sediments

Squared particles, low concentration



Small, elongated particles, high concentration



**Fig. 4 Proposed fire regimes scenarios obtained from the analysis of microcharcoal types and concentration produced and deposited in the marine environment off Africa.** The forested ecosystem of central western Africa is dominated by small and low-intensity fires producing squared microcharcoal particles in low concentration. Intense and large fires are specific for southern Africa with fires burning graminoid-mixed vegetation and producing small, elongated particles in high concentration. The figure was created in Affinity Designer 1.10.

twenty-one less than 150 years, twenty-four less than 200 years, fifteen less than 500 years and twelve of several hundred years up to late Holocene, and six samples of Holocene age. We were unable to date some core-top samples using the  $^{210}\text{Pb}$  method since some of the marine sediment cores were collected during oceanographic cruises from the 1990s. The ages of 46 core-top samples are based on direct chronologies of the sediment cores. The ages of 13 samples were inferred from closeby cores with direct chronologies. The year of the collection was assigned to one sample from the estuary and to 4 samples from multi-cores that preserved the sediment-water interface (presence of the oxic layer). For the other 4 samples that had no closeby cores with direct chronologies, we assigned a Holocene age based on foraminifera assemblages or benthic oxygen isotopic measurements. For the remaining 60 samples located off the western and central Africa coast, we inferred their ages from published sedimentation rates in multiple cores surrounding our samples<sup>63,64</sup> (please see Data availability). The study of<sup>64</sup> presents means terrigenous fluxes ( $\text{g}/\text{cm}^3/\text{ka}$ ) during the Late Quaternary. We calculated the sedimentation rates by dividing the terrigenous flux by the dry density ( $\text{g}/\text{cm}^3$ ), using a dry density of  $0.776 \text{ g}/\text{cm}^3$  (estimated using a humid density of  $1.5 \text{ g}/\text{cm}^3$ , and a 2.65 grain density and a 0.707 porosity). For each sample, we estimated a maximum average sedimentation rate from which we inferred the largest estimated ages (calendar years). We assumed that the range of estimated ages includes age uncertainties.

Studies<sup>65</sup> show that core-top of marine sediments represents the late Holocene and covers few hundred to few thousand years which might be problematic in terms of comparison with more recent observations. However, prior studies have successfully used spatial calibration of marine surface sediment-based proxies to reconstruct different physical and biological ocean and sea-ice properties (for example<sup>66–70</sup>) or fire regime characteristics<sup>27</sup> suggesting that core-top samples are suitable for our calibration approach. In particular, a study using core-top sediments off Iberia<sup>27</sup> showed that the temporal variability of microcharcoal concentrations in interface cores off Iberia is within the range of modern spatial variability. This supports our comparison of the different datasets as mean environmental conditions on land and in the ocean over the past 100 years, corresponding to these past century biomass burning records, did not radically depart from conditions recorded by the instrumental period. For the development of future calibration studies, it is recommended to focus on sediment samples collected with a multitube corer device that preserves the mud-water interface.

**Sample preparation.** Charcoal particles are produced at temperatures ranging between  $200^\circ$  to  $600^\circ\text{C}$ <sup>52</sup>. They are inorganic carbon, thus inert and resistant to biological and chemical decomposition<sup>29</sup>. The microcharcoal preparation techniques were adapted from previous work<sup>71</sup>, classical palynology methods<sup>72</sup> and petrographic mounted slides<sup>73</sup>. Microcharcoal samples were processed following the sediment preparation protocol previously published<sup>74</sup> slightly modified depending on the composition (organic-, silica-, carbonate-rich) of marine surface sediment samples. The microcharcoal extraction technique was applied to approximately 0.2 g of dried bulk sediment and consisted of the following steps: (a) a chemical treatment of hydrochloric acid (37% HCl) to remove calcium carbonates ( $\text{CaCO}_3$ ) until the reaction, i.e., degassing bubbles, stopped; (b) followed by nitric acid (68%  $\text{HNO}_3$ ) and hydrogen peroxide (33%  $\text{H}_2\text{O}_2$ ) attack on warm water-bath to remove or bleach the organic matter; (c) centrifugation to remove the supernatant before; (d) a chemical attack of hydrofluoric acid (HF) to remove siliceous material followed by centrifugation to remove HF; (e) followed by an HCl

treatment to remove colloidal  $\text{SiO}_2$  and silicofluorides formed during the HF digestion followed by a centrifugation to remove HCl. For samples with more than 1% organic matter, we added additional steps with alternating nitric acid and hydrogen peroxide chemical attack. This chemical treatment is used to remove carbonates, pyrites, humic material, labile or less refractory organic matter (OM), to bleach non-oxidized OM and to remove silicates. A dilution of 0.1 is applied to the residue. The suspension was then filtered onto a membrane of  $0.45 \mu\text{m}$  porosity. A portion of this membrane was mounted onto a Polymethyl Methacrylate (PMMA) slide with ethyl acetate before gentle polishing with alumin powder. The microscopic charcoal particles were identified under oil immersion using petrographic criteria in reflected light. The microcharcoal quantification was performed in transmitted light using image analysis (Leica DM6000 microscope and LAS software). Only charcoal particles  $>10 \mu\text{m}$  were analyzed. Previous work<sup>75</sup> reported some fragmentation of particles when using  $\text{HNO}_3$  or  $\text{H}_2\text{O}_2$  on modern charcoal and on peat sediment containing charcoal. The microcharcoal concentration (CCnb representing the number of microcharcoal particles per gram of dry weight sediment) and microcharcoal surface area (CCsurf, representing the sum of all surfaces of microcharcoal particles in one sample per gram) are significantly and positively correlated (Supplementary Fig. 7,  $r=0.86$ ,  $p<0.01$ ), suggesting that potential fragmentation due the chemical procedure<sup>75</sup> is minimal. Both parameters record the same pattern of microcharcoal variability highlighting that CCnb can be used here to inform about these changes. A bias in our charcoal record might come from the use of  $\text{H}_2\text{O}_2$  that may bleach or remove partially charred particles resulting from low temperature fires<sup>76</sup>. To minimize the error, we followed their recommendations by using solutions of consistent strength to treat all samples.

**Geographic information system (GIS): continent, ocean and fire data.** Information about the hydrographic basins was extracted from Natural Earth Data and GRIN database<sup>77</sup>. The characteristics of the hydrographic basins (size, hypsometry, river network) were extracted from the ASTER Global Digital Elevation Model free dataset.

The information regarding vegetation type was extracted from European Space Agency (ESA) Climate Change Initiative (CCI) Land Cover (LC) database<sup>77</sup>. The twenty-eight land cover classes from this database<sup>77</sup> were reclassified into 3 major growth habitat categories: graminoid including non-forested land cover types, mixed including mosaic land cover type and closed including forested types (Fig. 1a, Supplementary Table 2). The other land cover types were included in the not-burning (NB) category (Fig. 1a, Supplementary Table 2).

Fire regimes characteristics, including fire number, fire area, fire intensity (mean fire radiative power), rate of spread (derived from fire size and duration) and the three most important types of burnt vegetation (according to global Land Cover Climate Change Initiative, CCI-LC) were extracted from the global fire patch database FRY (2001–2019)<sup>41,78</sup>, updated with the newly delivered FireCCI51 250 m resolution pixel-level burn dates<sup>79</sup>. We used the mean FRP ( $\text{Watt}/\text{m}^2$ ) as a measure of fire intensity; FRP measures the energy emitted through radiative processes released during the combustion and can be associated with fire intensity all throughout the fire-burning process<sup>78</sup>. FRP is used for assessing carbon emissions by converting FRP into fuel biomass consumption rate<sup>80</sup>. FRP is also a key component of global fire regime characterization<sup>81</sup>. For ease of interpretation, the most important burnt vegetation classes (L1, L2, L3) provided in FRY v2 were translated into 3 land cover classes according to

the vegetation growth habitat they were spreading into (Supplementary Table 2). We used this reclassification to have the same level of information from land fire data and charcoal from the sediment records and examine the relationship between them. The information on fire patches from FRY v2 were aggregated on a  $1^\circ \times 1^\circ$  grid for each hydrographic basin by calculating the median of the number of fire patches (>100 ha), burned area, FRP and RoS per vegetation type.

**Modelling the dispersion of fire plumes and charcoal particles deposition.** The Hybrid Single-Particle Lagrangian Integrated Trajectory model (HYSPLIT)<sup>82</sup> plume dispersion model and computation of particle concentration was used to simulate the dispersion of fire plumes and deposition of charcoal particles in our attempt to estimate the most likely airborne charcoal source area. Based on the physics of particles, this simulation uses a fixed number of particles which are transported by a wind field, spread by a turbulent component and, in our case, removed by dry and wet mechanisms<sup>82</sup>. For this simulation we used meteorological fields from National Centers for Environmental Prediction's (NCEP) Global Data Assimilation Scheme (GDAS) with  $1^\circ \times 1^\circ$  resolution and 3-hourly data covering the interval 2007 to present.

We tested the Hysplit air dispersal and deposition model in ten fire locations, for three atmospheric levels and three micro-charcoal particles sizes that describe the range of our dataset (SI Section 3). Details regarding parametrization and test simulation are provided in SI Section 3. The results were similar in most fire locations showing that the distance traveled by the particles, regardless of their size and atmospheric level, is directly proportional with the injection height and most of the microscopic charcoal stays within a few tens to a few hundreds of kilometers (Supplementary Table 1) from the fire area. From spatial charcoal concentration maps (Supplementary Fig. 3 maps and Supplementary Table 1) wind and fluvial source areas overlap so that most of charcoal produced in one hydrographic basin is deposited in the same basin and can then be transported to the ocean by the fluvial system. Considering the closed land-sea link between pollen assemblages and latitudinal vegetation distribution in Africa<sup>37</sup>, we anticipate microcharcoal deposited in marine sediments come from the closest hydrographic basins and reflect spatial fire regimes distribution.

We therefore used the limits of the hydrographic basins and distance from the river mouth and coast to identify the closest source-areas. Samples located within the Congo system (using the oceanographic limits) were assigned to Congo hydrographic basin. We obtained eight zones as follow, from N to S: Gulf of Guinea (31 samples), Congo (72 samples), Angola (14 samples), Namibia (4 samples), Orange (2 samples), western South Africa (4 samples), Eastern South Africa (4 samples) and Limpopo (1 sample) (Fig. 1a).

**Statistical analysis.** A set of statistical analyses were run and visualized in Rstudio Version 1.3.1093<sup>83</sup> using packages Tidyverse, FactoMineR and Factoextra. Principal Component Analysis (PCA), centered and scaled, was used to assess the potential clustering of charcoal particle types, including their area, length, width, elongation (length-to-width ratio) by hydrographic basins. We used squared cosine (cos<sup>2</sup>) to determine the quality of representation and strength of the relationship for each variable on the dimension. The same analysis was applied to land fire parameters, including the number of fires, fire radiative power (FRP), area, rate of spread (RoS) and the burnt vegetation types (graminoid - G, mixed - M, trees - T) to characterize the fire parameters specific for hydrographic basins. Given the high

number of satellite observations, before running the analysis, the median of fire regime parameters was calculated per grid cell. Kruskal–Wallis rank sum test (KW test, `kruskal.test()` function, R cran) was applied on PC1 values of ocean charcoal and land fire data to determine whether there is a significant difference among hydrographic basin distribution on the PCA driven by charcoal parameters for the ocean data set, and land fire parameters for the land data set. The KW test was also run to determine the statistical differences among regions, western central versus Southern Africa. Bilateral student t-test were performed on the elongation dataset to determine the mean differences between hydrographic basins, `t.test()` function, R cran.

### Data availability

The dataset generated for this study is available in the [https://figshare.com/articles/dataset/Microcharcoal\\_dataset\\_of\\_surface\\_ocean\\_sediments\\_offshore\\_Africa/22566901](https://figshare.com/articles/dataset/Microcharcoal_dataset_of_surface_ocean_sediments_offshore_Africa/22566901) repository.

Received: 3 August 2022; Accepted: 6 April 2023;

Published online: 22 April 2023

### References

- Bowman, D. M. J. S. et al. Fire in the earth system. *Science* **324**, 481–484 (2009).
- Pausas, J. G. & Keeley, J. E. A burning story: the role of fire in the history of life. *Bioscience* **59**, 593–601 (2009).
- McLauchlan, K. K. et al. Fire as a fundamental ecological process: research advances and frontiers. *J. Ecol.* **108**, 2047–2069 (2020).
- van der Werf, G. R. et al. Global fire emissions and the contribution of deforestation, savanna, forest, agricultural, and peat fires (1997–2009). *Atmos. Chem. Phys.* **10**, 11707–11735 (2010).
- Pfeiffer, M., Spessa, A. & Kaplan, J. O. A model for global biomass burning in preindustrial time: LPJ-LMfire (v1.0). *Geosci. Model Dev.* **6**, 643–685 (2013).
- Moritz, M. A. et al. Climate change and disruptions to global fire activity. *Ecosphere* **3**, 1–22 (2012).
- Pechony, O. & Shindell, D. T. Driving forces of global wildfires over the past millennium and the forthcoming century. *Proc. Natl. Acad. Sci.* **107**, 19167–19170 (2010).
- Hantson, S. et al. Fire in the earth system - bridging data and modelling research. *B. Am. Meteorol. Soc.* **97**, 1069–1072 (2016).
- Giglio, L. et al. Assessing variability and long-term trends in burned area by merging multiple satellite fire products. *Biogeosciences* **7**, 1171–1186 (2010).
- Mouillot, F. & Field, C. B. Fire history and the global carbon budget: a  $1^\circ \times 1^\circ$  fire history reconstruction for the 20th century. *Global Change Biol.* **11**, 398–420 (2005).
- Hawthorne, D. et al. Global modern charcoal dataset (GMCD): a tool for exploring proxy-fire linkages and spatial patterns of biomass burning. *Quatern Int.* **488**, 3–17 (2018).
- Marlon, J. R. et al. Global biomass burning: a synthesis and review of Holocene paleofire records and their controls. *Quat. Sci. Rev.* **65**, 5–25 (2013).
- Marlon, J. R. et al. Reconstructions of biomass burning from sediment-charcoal records to improve data–model comparisons. *Biogeosciences* **13**, 3225–3244 (2016).
- Adolf, C. et al. The sedimentary and remote-sensing reflection of biomass burning in Europe. *Global Ecol. Biogeogr.* **27**, 199–212 (2018).
- Duffin, K. I., Gillson, L. & Willis, K. J. Testing the sensitivity of charcoal as an indicator of fire events in savanna environments: quantitative predictions of fire proximity, area and intensity. *Holocene* **18**, 279–291 (2008).
- Hennebelle, A. et al. The reconstruction of burned area and fire severity using charcoal from boreal lake sediments. *Holocene* **30**, 1400–1409 (2020).
- Higuera, P. E., Peters, M. E., Brubaker, L. B. & Gavin, D. G. Understanding the origin and analysis of sediment-charcoal records with a simulation model. *Quat. Sci. Rev.* **26**, 1790–1809 (2007).
- Ley, B., Brewer, S. C., McConaghy, S., Mueller, J. & McLauchlan, K. K. Fire history reconstruction in grassland ecosystems: amount of charcoal reflects local area burned. *Environ. Res. Lett.* **10**, 114009 (2015).
- Higuera, P. E., Whitlock, C. & Gage, J. A. Linking tree-ring and sediment-charcoal records to reconstruct fire occurrence and area burned in subalpine forests of Yellowstone National Park, USA. *Holocene* **21**, 327–341 (2011).
- Shen, Y. et al. Reconstructing burnt area during the Holocene: an Iberian case study. *Clim. Past Discuss* **2021**, 1–23 (2021).

21. Tinner, W. et al. Pollen and charcoal in lake sediments compared with historically documented forest fires in southern Switzerland since AD 1920. *Holocene* **8**, 31–42 (1998).
22. Higuera, P. E., Sprugel, D. G. & Brubaker, L. B. Reconstructing fire regimes with charcoal from small-hollow sediments: a calibration with tree-ring records of fire. *Holocene* **15**, 238–251 (2005).
23. Daniau, A.-L. et al. Orbital-scale climate forcing of grassland burning in southern Africa. *Proc. Natl. Acad. Sci.* **110**, 5069–5073 (2013).
24. Dupont, L. M. & Schefuß, E. The roles of fire in Holocene ecosystem changes of West Africa. *Earth Planet Sci. Lett.* **481**, 255–263 (2018).
25. Dupont, L. M., Zhao, X., Charles, C., Faith, J. T. & Braun, D. Continuous vegetation record of the Greater Cape Floristic Region (South Africa) covering the past 300 000 years (IODP U1479). *Clim. Past* **18**, 1–21 (2021).
26. Mensing, S. A., Michaelsen, J. & Byrne, R. A 560-year record of santa ana fires reconstructed from charcoal deposited in the Santa Barbara Basin, California. *Quat. Res.* **51**, 295–305 (1999).
27. Genet, M. et al. Modern relationships between microscopic charcoal in marine sediments and fire regimes on adjacent landmasses to refine the interpretation of marine paleofire records: an Iberian case study. *Quat. Sci. Rev.* **270**, 107148 (2021).
28. Herring, J. R. The carbon cycle and atmospheric CO<sub>2</sub>: natural variations archean to present. *Geophys. Monogr. Ser.* 419–442 <https://doi.org/10.1029/gm032p0419> (1985).
29. Patterson, W. A., Edwards, K. J. & Maguire, D. J. Microscopic charcoal as a fossil indicator of fire. *Quat. Sci. Rev.* **6**, 3–23 (1987).
30. Whitlock, C. & Larsen, C. Tracking environmental change using lake sediments, terrestrial, algal, and siliceous indicators. *Dev. Paleoenvir. Res.* 75–97 [https://doi.org/10.1007/0-306-47668-1\\_5](https://doi.org/10.1007/0-306-47668-1_5) (2002).
31. Clark, J. S., Lynch, J., Stocks, B. J. & Goldammer, J. G. Relationships between charcoal particles in air and sediments in west-central Siberia. *Holocene* **8**, 19–29 (1998).
32. Heusser, L. E. Pollen distribution in the bottom sediments of the western North Atlantic Ocean. *Mar. Micropaleontol.* **8**, 77–88 (1983).
33. Mudie, P. J. & McCarthy, F. M. G. Marine palynology: potentials for onshore—offshore correlation of Pleistocene—Holocene records. *T Roy Soc. S. Afr.* **61**, 139–157 (2006).
34. Dupont, L. Orbital scale vegetation change in Africa. *Quat. Sci. Rev.* **30**, 3589–3602 (2011).
35. Hooghiemstra, H., Lézine, A.-M., Leroy, S. A. G., Dupont, L. & Marret, F. Late Quaternary palynology in marine sediments: a synthesis of the understanding of pollen distribution patterns in the NW African setting. *Quat. Int.* **148**, 29–44 (2006).
36. Dupont, L. M. Use of proxies in paleoceanography, examples from the South Atlantic. 523–546 [https://doi.org/10.1007/978-3-642-58646-0\\_22](https://doi.org/10.1007/978-3-642-58646-0_22) (1999).
37. Dupont, L. M. & Wyputt, U. Reconstructing pathways of aeolian pollen transport to the marine sediments along the coastline of SW Africa. *Quat. Sci. Rev.* **22**, 157–174 (2003).
38. Goñi, M. F. S. et al. Pollen from the deep-sea: a breakthrough in the mystery of the ice ages. *Front Plant Sci.* **9**, 38 (2018).
39. Daniau, A.-L. et al. Terrestrial plant microfossils in palaeoenvironmental studies, pollen, microcharcoal and phytolith. Towards a comprehensive understanding of vegetation, fire and climate changes over the past one million years. *Revue De Micropaléontologie* **63**, 1–35 (2019).
40. Vachula, R. S. A meta-analytical approach to understanding the charcoal source area problem. *Palaeogeogr. Palaeoclim. Palaeoecol.* **562**, 110111 (2021).
41. Laurent, P., Mouillot, F., Moreno, M. V., Yue, C. & Ciais, P. Varying relationships between fire radiative power and fire size at a global scale. *Biogeosciences* **16**, 275–288 (2018).
42. Aleman, J. C. et al. Tracking land-cover changes with sedimentary charcoal in the Afrotropics. *Holocene* **23**, 1853–1862 (2013).
43. Umbanhowar, C. E. & McGrath, M. J. Experimental production and analysis of microscopic charcoal from wood, leaves and grasses. *Holocene* **8**, 341–346 (1998).
44. Mastrolonardo, G. et al. Size fractionation as a tool for separating charcoal of different fuel source and recalcitrance in the wildfire ash layer. *Sci. Total Environ.* **595**, 461–471 (2017).
45. van Leeuwen, T. T. et al. Biomass burning fuel consumption rates: a field measurement database. *Biogeosciences* **11**, 7305–7329 (2014).
46. Hantson, S. et al. Rare, Intense, Big fires dominate the global tropics under drier conditions. *Sci. Rep. UK* **7**, 14374 (2017).
47. Marlon, J., Bartlein, P. J. & Whitlock, C. Fire-fuel-climate linkages in the northwestern USA during the Holocene. *Holocene* **16**, 1059–1071 (2006).
48. Smith, D. M., Griffin, J. J. & Goldberg, E. D. Elemental carbon in marine sediments: a baseline for burning. *Nature* **241**, 268–270 (1973).
49. Ward, D. E. et al. Effect of fuel composition on combustion efficiency and emission factors for African savanna ecosystems. *J. Geophys. Res. Atmos.* **101**, 23569–23576 (1996).
50. Blackford, J. J. Charcoal fragments in surface samples following a fire and the implications for interpretation of subfossil charcoal data. *Palaeogeogr. Palaeoclim. Palaeoecol.* **164**, 33–42 (2000).
51. Lynch, J. A., Clark, J. S. & Stocks, B. J. Charcoal production, dispersal, and deposition from the Fort Providence experimental fire: interpreting fire regimes from charcoal records in boreal forests. *Can. J. Forest Res.* **34**, 1642–1656 (2004).
52. Conedera, M. et al. Reconstructing past fire regimes: methods, applications, and relevance to fire management and conservation. *Quat. Sci. Rev.* **28**, 555–576 (2009).
53. Feurdean, A. Experimental production of charcoal morphologies to discriminate fuel source and fire type: an example from Siberian taiga. *Biogeosciences* **18**, 3805–3821 (2021).
54. Vachula, R. S., Sae-Lim, J. & Li, R. A critical appraisal of charcoal morphometry as a paleofire fuel type proxy. *Quat. Sci. Rev.* **262**, 106979 (2021).
55. Crawford, A. J. & Belcher, C. M. Charcoal morphometry for paleoecological analysis: the effects of fuel type and transportation on morphological parameters. *Appl. Plant Sci.* **2**, apps.1400004 (2014).
56. Archibald, S., Lehmann, C. E. R., Gómez-Dans, J. L. & Bradstock, R. A. Defining pyromes and global syndromes of fire regimes. *Proc. Natl. Acad. Sci.* **110**, 6442–6447 (2013).
57. Congolobe, et al. The Congolobe project, a multidisciplinary study of Congo deep-sea fan lobe complex: Overview of methods, strategies, observations and sampling. *Deep Sea Res. Part II Top Stud. Oceanogr.* **142**, 7–24 (2017).
58. Cochonat. ZAIANGO2 cruise, RV L'Atalante. <https://doi.org/10.17600/98010110> (1998).
59. Savoye, B. & Ondreas, H. ZAIANGOROV cruise, RV L'Atalante., <https://doi.org/10.17600/10100> (2000).
60. Savoye, B. ZAIANGO1 cruise, RV L'Atalante. <https://doi.org/10.17600/98010100> (1998).
61. deBaar, H. & al., et. JGOFS North Atlantic R.V. Tyro Leg 2 of the cruise in 1989, *Upper Ocean Processes.* (1989).
62. Bertrand, P. NAUSICAA — Images II MD 105 Cruise Report. Institut Français pour la Recherche et la Technologie Polaire (IFRTP). (1997).
63. Baudin, F. et al. Organic carbon accumulation in modern sediments of the Angola basin influenced by the Congo deep-sea fan. *Deep Sea Res. Part II Top Stud. Oceanogr.* **142**, 64–74 (2017).
64. Jansen, J. H. F., Weering, T. C. E. V., Gieles, R. & Iperen, J. V. Middle and late quaternary oceanography and climatology of the Zaire-Congo fan and the adjacent Eastern Angola basin. *Neth. J. Sea Res.* **17**, 201–249 (1984).
65. Müller, P. J., Kirst, G., Ruhland, G., von Storch, I. & Rosell-Melé, A. Calibration of the alkenone paleotemperature index U<sub>37K'</sub> based on core-tops from the eastern South Atlantic and the global ocean (60°N–60°S). *Geochim. Cosmochim. Acta* **62**, 1757–1772 (1998).
66. Radi, T. & de Vernal, A. Dinocysts as proxy of primary productivity in mid-high latitudes of the Northern Hemisphere. *Mar. Micropaleontol.* **68**, 84–114 (2008).
67. Kucera, M. et al. Reconstruction of sea-surface temperatures from assemblages of planktonic foraminifera: multi-technique approach based on geographically constrained calibration data sets and its application to glacial Atlantic and Pacific Oceans. *Quat. Sci. Rev.* **24**, 951–998 (2005).
68. Dupont, L. M., Behling, H., Jahns, S., Marret, F. & Kim, J.-H. Variability in glacial and Holocene marine pollen records offshore from west southern. *Afr. Veg. Hist. Archaeobot* **16**, 87–100 (2007).
69. Hessler, I. et al. Millennial-scale changes in vegetation records from tropical Africa and South America during the last glacial. *Quat. Sci. Rev.* **29**, 2882–2899 (2010).
70. Hardy, W. et al. Quantification of last glacial-Holocene net primary productivity and upwelling activity in the equatorial eastern Atlantic with a revised modern dinocyst database. *Palaeogeogr. Palaeoclim. Palaeoecol.* **505**, 410–427 (2018).
71. Winkler, M. G. Charcoal analysis for paleoenvironmental interpretation: a chemical assay. *Quat. Res.* **23**, 313–326 (1985).
72. Beaufort, L., de Garidel-Thoron, T., Linsley, B., Oppo, D. & Buchet, N. Biomass burning and oceanic primary production estimates in the Sulu Sea area over the last 380 kyr and the East Asian monsoon dynamics. *Mar. Geol.* **201**, 53–65 (2003).
73. Daniau, A.-L., Goñi, M. F. S. & Duprat, J. Last glacial fire regime variability in western France inferred from microcharcoal preserved in core MD04-2845, Bay of Biscay. *Quat. Res.* **71**, 385–396 (2009).
74. Daniau, A.-L. et al. Dansgaard-Oeschger climatic variability revealed by fire emissions in southwestern Iberia. *Quat. Sci. Rev.* **26**, 1369–1383 (2007).
75. Tsakiridou, M., Cunningham, L. & Hardiman, M. Toward a standardized procedure for charcoal analysis. *Quat. Res.* **99**, 329–340 (2021).
76. Schlachter, K. J. & Horn, S. P. Sample preparation methods and replicability in macroscopic charcoal analysis. *J. Paleolimnol.* **44**, 701–708 (2010).

77. ESA. *Land Cover CCI Product User Guide Version 2. Tech. Rep.* [maps.elie.ucl.ac.be/CCI/viewer/download/ESACCI-LC-Ph2-PUGv2\\_2.0.pdf](https://maps.elie.ucl.ac.be/CCI/viewer/download/ESACCI-LC-Ph2-PUGv2_2.0.pdf) (2014).
78. Laurent, P. et al. FRY, a global database of fire patch functional traits derived from space-borne burned area products. *Sci. Data* **5**, 180132 (2018).
79. Chuvieco, E. et al. Generation and analysis of a new global burned area product based on MODIS 250 m reflectance bands and thermal anomalies. *Earth Syst. Sci. Data* **10**, 2015–2031 (2018).
80. Kaiser, J. W. et al. Biomass burning emissions estimated with a global fire assimilation system based on observed fire radiative power. *Biogeosciences* **9**, 527–554 (2012).
81. García, M. et al. Characterizing global fire regimes from satellite-derived products. *Forests* **13**, 699 (2022).
82. Stein, A. F. et al. NOAA's HYSPLIT atmospheric transport and dispersion modeling system. *B Am. Meteorol. Soc.* **96**, 2059–2077 (2015).
83. Team, R. C. A language and environment for statistical computing. *R Found. Statistical Comput.* <https://www.R-project.org/> (2021).

## Acknowledgements

This work was supported by the ANR BRAISE project, grant ANR-19-CE01-0001-01 of the French Agence Nationale de la Recherche; French INSU (Institut National des Sciences de l'Univers) programme LEFE (Les Enveloppes Fluides et l'Environnement) CAMPFIRE project; and by the Climate Change Initiative (CCI) Fire\_cci Project (Contract 4000126706/19/I-NB). We acknowledge M. Georget and L. Devaux for their technical help.

## Author contributions

A.H., A-L.D. designed research and interpreted data; A.H. collected and analyzed the data; F.M., W.C. contributed new fire satellite data; B.L. and V.D. advised on statistical analyses; B.D., E.S., G.B., X.C. provided access to surface samples; A.H., A-L.D., F.M., W.C., B.L., V.D., V.H., B.D., E.S., G.B., X.C. contributed to the manuscript writing; A.H., A-L.D. lead the manuscript.

## Competing interests

The authors declare no competing interests.

## Additional information

**Supplementary information** The online version contains supplementary material available at <https://doi.org/10.1038/s43247-023-00800-x>.

**Correspondence** and requests for materials should be addressed to Aritina Haliuc or Anne-Laure Daniau.

**Peer review information** *Communications Earth & Environment* thanks Fabienne Marret-Davies, Mitchell Power and the other, anonymous, reviewer(s) for their contribution to the peer review of this work. Primary Handling Editor: Aliénor Lavergne. Peer reviewer reports are available.

**Reprints and permission information** is available at <http://www.nature.com/reprints>

**Publisher's note** Springer Nature remains neutral with regard to jurisdictional claims in published maps and institutional affiliations.



**Open Access** This article is licensed under a Creative Commons Attribution 4.0 International License, which permits use, sharing, adaptation, distribution and reproduction in any medium or format, as long as you give appropriate credit to the original author(s) and the source, provide a link to the Creative Commons license, and indicate if changes were made. The images or other third party material in this article are included in the article's Creative Commons license, unless indicated otherwise in a credit line to the material. If material is not included in the article's Creative Commons license and your intended use is not permitted by statutory regulation or exceeds the permitted use, you will need to obtain permission directly from the copyright holder. To view a copy of this license, visit <http://creativecommons.org/licenses/by/4.0/>.

© The Author(s) 2023